Green Chemistry

Accepted Manuscript

This article can be cited before page numbers have been issued, to do this please use: H. Bergem, R. Xu, R. C. Brown and G. Huber, *Green Chem.*, 2017, DOI: 10.1039/C7GC00367F.

ROYAL SOCIETY OF CHEMISTRY

rsc.li/green-chem

View Article Online
DOI: 10.1039/C7GC00367F

Low Temperature Aqueous Phase Hydrogenation of the Light Oxygenate Fraction of Bio-oil over Supported Ruthenium Catalysts

Håkon Bergem[1] , Run Xu[2] , Robert C. Brown[3] and George W. Huber[4]

[1] Department of Oil and Gas Process Technology, SINTEF Materials & Chemistry, N-7465, Trondheim, Norway
[2] Hydroprocessing Department, Research Institute of Petroleum Processing, Sinopec, 18 Xueyuan Road, P.O. Box 914-17, Beijing 100083, P.R. China
[3] Department of Mechanical Engineering, Iowa State University, Ames, IA 50011, USA
[4] Department of Chemical and Biological Engineering, University of Wisconsin-Madison, 1415 Engineering Drive, Madison, WI 53706, USA

Abstract

The low temperature hydrogenation of light oxygenates in the aqueous fraction of bio-oil (AFBO) was studied using both model compounds and a real bio-oil fraction with Ru/TiO_2 and Ru/C catalysts in a continuous flow reactor. Hydrogenation of hydroxyacetone, acetic acid, and formic acid, in single and multi-compound aqueous mixtures produced 1,2-propanediol, ethanol, and CO_2 respectively, as the main products. The addition of acetic acid increased the rate of hydrogenation of hydroxyacetone by catalyzing the enolization of hydroxyacetone. The main reactions occurring during hydrogenation of the light oxygenates in the aqueous fraction bio-oil included conversion of hydroxy-ketones into diols and hydrogenation of ketones and aldehydes into mono-alcohols. Differences in the product selectivity between the model carboxylic acids and APBO were observed. High selectivity to ethanol was found when model-feed mixtures containing acetic acid were hydrogenated. In contrast the ethanol selectivity for hydrotreating of the APBO was 13 times lower than the ethanol selectivity for hydrotreating of acetic acid in water. A declining catalyst activity was observed when processing the APBO.

Keywords: bio-oil upgrading, light oxygenates, aqueous phase hydrogenation, biochemicals

View Article Online
DOI: 10.1039/C7GC00367F

1.0 Introduction

Fast pyrolysis is becoming one of the most promising technologies for harvesting solar energy stored in biomass by thermochemically transforming it into a high energy density liquid product [1-4]. There are numerous advantages of handling liquid fuels in terms of transportation, storage, transfer, and further chemical processing. The existing infrastructure for fossil derived-liquid fuels makes the utilization of liquid fuels derived from renewable resources an obvious choice.

Bio-oil from fast pyrolysis of biomass consists of a large number of chemical compounds in the form of oxygenated organic molecules and water. The oxygenated compounds that are found in bio-oil include pyrolytic lignin (phenolic oligomers), acetic acid, hydroxyacetone, hydroxyacetaldehyde, anhydrosugars, furans, and several other oxygenated compounds. Bio-oil polymerizes upon heating and therefore traditional methods like distillation cannot be used for separation [1]. Bio-oil has high oxygen content (up to 50 wt%), high acidity, and phase separates in storage. The vast number of chemical components in bio-oil makes targeted molecular alterations of the whole bio-oil by catalytic hydroprocessing non-selective. The products include large amounts of coke, tar, and light gases. Catalysts deactivate in the hydroprocessing of bio-oils as reported due to the high reactivity of aldehydes and ketones [5, 6]. Elliot et al. have reported on the beneficial effect on bio-oil stability by initially hydrogenating these compounds at low temperatures [7]. Stabilized bio-oil can subsequently be processed at higher temperatures and hydrogen pressure [7]. Furthermore, light oxygenates in the bio-oil will produce undesired methane and ethane when hydroprocessing bio-oil with conventional catalysts. Bio-oil contains around 25 wt% (dry basis) of light oxygenates (aldehydes, ketones, alcohols, and carboxylic acids) [8]. It would be highly desirable to convert all of these into alcohols or polyols.

View Article Online
DOI: 10.1039/C7GC00367F

A different approach is to recover the bio-oil from fast pyrolysis by selective condensation of different fractions in distinct stage fractions [9, 10]. These different fractions have distinctive physical and chemical characteristics. Tailored catalytic processes can then be designed for conversion of these unique fractions. The need for a combination of separation and conversion steps as a strategy in bio-oil upgrading is highlighted in a recent review by Resasco and Crossley [11]. The AFBO contains light oxygenates (C_1-C_6) with functionalities that can be tuned by hydrogenation into chemicals with desirable properties. Resasco et. al have also discussed the strategy of eliminating the small acids from bio-oil by aqueous phase ketonization producing larger ketones which subsequently can be hydrogenated into alcohols [12]. These alcohols can then be used to alkylate with phenolic compounds. The same group showed that the hydrogenation and alkylation step can be performed in a single reactor with two sequential catalyst beds [13]. Several investigations have shown that an array of chemicals including H_2, alkanes, and alcohols can be produced by aqueous phase processing of bio-oil [14-16].

Because of the resemblance between hydroprocessing of petroleum and bio-oils, several studies involving conventional CoMo and NiMo-catalysts have been conducted. Early work has been comprehensively reviewed [2, 17-21]. Compared to hydroprocessing of petroleum, upgrading of bio-oils requires lower Liquid Hourly Space Velocity (LHSV), higher pressure, higher H_2-consumption, and is substantially more exothermic. In addition catalyst stability for hydrodeoxygenation (HDO) of bio-oil is poor compared to hydrotreating of petroleum. Hydrotreating catalysts typically possess their highest activity for HDO in their sulfide form, but bio-oils do not contain sufficient levels of sulfur to maintain the catalyst structure in the desired sulfided state during operation. The catalyst support constitutes high surface area Al_2O_3 and water combined with high temperature is known to induce sintering and structural changes forming the hydroxide form (Boehmite) [18]. The presence of acidic sites on the

View Article Online
DOI: 10.1039/C7GC00367F

Al_2O_3-support in combination with potential coke precursors in the bio-oil also initiates polymerization/condensation reactions resulting in blocking of active sites by carbonaceous materials. Development of new catalyst formulations are needed to enable cost-efficient upgrading of bio-oil feedstocks.

Supported ruthenium catalysts have received increased attention as active and selective catalysts for the hydrogenation and HDO of oxygenated compounds [22-26] and bio-oil [27, 28]. Ru-metal on carbon or TiO_2 gives active catalysts that are hydrothermally stable under the reaction conditions. An additional advantage of utilizing TiO_2 in a commercial process is that oxidative regeneration of a deactivated catalyst would be possible while this is not possible in the case of carbon.

The objective of this paper is to study the low temperature aqueous phase hydrogenation (APH) of a staged bio-oil fraction containing light oxygenates over supported ruthenium catalysts to gain insight into the molecular level chemical reactions taking place. In addition, we will identify the effects of reaction conditions (temperature and contact time) on the product distribution. Experiments with single- and multi-component model-feeds in a continuous flow reactor have been performed to identify the reaction pathways for some of the main compounds in the real bio-oil and the mutual effect they impose on each other`s reactivity. Acetic acid (AA), hydroxyacetone (HA), and formic acid (FA) were chosen as representative of the light oxygenates found in the aqueous fraction of bio-oil collected through staged recovery of pyrolysis vapors as described by Pollard et al. [9] and Rover et al. [10]. Long-term catalyst stability when upgrading bio-oil is of particular importance because of carbon formation, poisoning from feed impurities, and leaching of active metal from the catalyst. This paper also provides increased knowledge on the production of value added chemicals from bio-oil feedstocks.

View Article Online
DOI: 10.1039/C7GC00367F

2. Experimental

2.1 Catalyst preparation and characterization

The 3 wt% Ru/TiO_2 catalyst was prepared by the incipient wetness method with ruthenium (III) nitrosyl nitrate (Sigma-Aldrich catalog number 373567, 1.5 wt% Ru in dilute nitric acid solution) as the Ru precursor. The titania was supplied by Sigma-Aldrich (catalog number 718467). The support was calcined at 400 °C for 4 h in a muffle furnace (heating rate 4 °C/h) prior to use. In the catalyst synthesis, a volume of the precursor containing Ru equivalent to 3 wt% of the weighted titania was added drop-wise to the support previously dried at 110 °C for 12 h until incipient wetness was observed. Multiple impregnation steps were needed with drying of the sample at 110 °C for 12 h after each step. The 5 wt% Ru/C was a commercial available catalyst (Strem Chemicals) and was used as received.

The Brunner-Emmett-Teller (BET) surface area of the catalysts was determined from N_2 physisorption at -196 °C using a Micromeritics ASAP 2020 system. Before the measurements, the sample was degassed under vacuum at 523 K for 12 h. The pore volume and average pore diameter for each catalyst were calculated by the Barrett–Joyner–Halenda (BJH) desorption method.

H_2 uptake of the catalysts were carried out at 50°C using a Micromeritics® AutoChem II 2920 system; each sample (200 mg) was reduced in situ at 450°C for 2 h at a heating rating of 1 °C min^{-1} in flowing hydrogen (50 mL min^{-1}) prior to chemisorption measurements. After the reduction was complete, the sample was degassed at 450°C for 2 h in He. The sample cell was cooled to 50°C. The peak area can be correlated with the amount of adsorbed H_2 on the basis of pulsed H_2 experiments. Surface average metal particle sizes were calculated using the equation

$$D = 6/S\rho,$$

View Article Online
DOI: 10.1039/C7GC00367F

where *S* is the metal surface area per gram of metal, and ρ the density of the metal. A cross-sectional area of 9.03 $Å^2$ per Ru surface atom was assumed for calculating *S* [29].

Temperature-programmed-reduction (TPR) of the Ru/TiO_2 catalyst was performed in a Micromeritics Autochem II 2920 instrument.

2.2 Preparation and characterization of model compounds and aqueous fraction of bio-oil

Model compounds used in this study included acetic acid (AA; purity > 99.7%), formic acid (FA; purity > 98%), and hydroxyacetone (HA; purity > 90%) supplied by Sigma-Aldrich and used without further purification.

Bio-oil was produced by pyrolyzing red oak at 500 °C in an 8 kg/h pyrolysis development unit (PDU) at Iowa State University's BioCentury Research Farm. This system has a bio-oil recovery system that separates bio-oil into distinctive stage fractions, as previously described by Rover et al. [9]. Heavy ends consisting of lignin-derived phenolic oligomers and carbohydrate-derived anhydrosugars were removed from the pyrolysis vapor stream by a condenser and electrostatic precipitator with coolant set to 85 °C; a middle fraction consisting of mostly furanics and phenolic monomers was removed by a second condenser and electrostatic precipitator with coolant set at 65 °C; the AFBO employed in the present study, consisting of water-soluble light oxygenates, was removed by a condenser operated at 18 °C. The aqueous fraction was stored in a refrigerator and filtered before use.

Inductively coupled plasma (ICP) analysis of the liquid products was performed on a Plasma 400 ICP (Perkin Elmer).

2.3 Aqueous phase hydrogenation

View Article Online
DOI: 10.1039/C7GC00367F

Aqueous-phase hydrogenation was performed in a continuous flow reactor operated in up-flow mode. The experimental setup was placed in a ventilated hood with a safety screen in front. All pressurized lines were equipped with safety relief valves and hydrogen was feed from a gas cylinder completed with an automatic shut-off valve (Hoke). The reactor consisted of a ¼ inch stainless steel tube 580 mm long with 3 mm inner diameter placed inside a furnace with an aluminum block/filler inserted in the void between the furnace and the tubular reactor. The aluminum filler was used to obtain a uniform temperature profile along the catalyst bed by improved heat transfer. In the experiments 2.0 g of catalyst was usually loaded into the reactor and positioned with glass wool above and below the catalyst bed. In the case of the extra-low temperature experiments with HA, 0.5 g of catalyst was used. Reduction of the catalyst was performed by feeding hydrogen at a flow rate of 100 mL min^{-1} while heating the reactor to 300 °C at a rate of 30 °C/h. The catalyst was soaked at 300 °C for 2 h before the temperature was decreased to room temperature before the pressure was increased to the operating pressure. The liquid was fed to the reactor by a Varian ProStar 210 HPLC pump and mixed with hydrogen before the reactor inlet. Hydrogen flow rate was 40 mL min^{-1} metered by a Brooks mass flow controller. The product mixture passed through a gas-liquid separator before the gas flowed through a back-pressure valve (Swagelok) maintaining the system pressure. Gaseous products were vented or periodically directed to an online gas chromatograph (Shimadzu GC-2014) by a three-way valve for composition analysis. Compound separation was obtained with two columns using helium as carrier gas. Hydrocarbons were separated on a RT-Q-Bond capillary column and analyzed with a flame ionization detector (FID) while permanent gases were separated on a ShinCarbon ST packed column and analyzed with a thermal conductivity detector (TCD).

Liquid products were sampled from the gas-liquid separator once every hour and analyzed offline by GC-FID, HPLC, GC-MS, and a Total Organic Carbon (TOC) analyzer. For the

View Article Online
DOI: 10.1039/C7GC00367F

experiments with model feeds at least 2 samples were collected at each set of operating conditions to ensure the steady state. The GC-FID was a Shimadzu GC-2010 with an Rtx-VMS capillary column utilizing helium as carrier gas. HPLC analysis was performed with a Shimadzu LC-20AT equipped with a Biorad Aminex HPX-87H column maintained at 30 °C and applying 0.005 M H_2SO_4 as the mobile phase pumped at 0.6 mL min^{-1}. Component detection was obtained with a UV-VIS detector (SPD-M20A) and a RI detector (RID-10A). The GC-MS-QP2010S (Shimadzu) was equipped with an Rtx-VMS capillary column using helium as carrier gas and a QP-2010. TOC was quantified using a Shimadzu TOC-VCPH analyzer.

3. Results and discussion

3.1 Characterization of catalysts

Physical properties of the prepared Ru catalysts are summarized in Table 1. The two support materials have distinctly different properties with carbon being a high surface area support (834 m^2/g) with a smaller average pore size (38.4 Å) compared to TiO_2 (57 m^2/g and 214.7 Å respectively). Hydrogen uptake on fresh Ru/C catalyst corresponds to a Ru dispersion of 7.8% or an average Ru particle size of 11.7 nm. Metal dispersion and average particle size on fresh Ru/TiO_2 catalyst were calculated to be 65.1% and 1.4 nm respectively. TPR of fresh Ru/TiO_2 catalyst showed one large peak with a maximum at 120 °C and a smaller shoulder peak with a maximum at 150 °C. No additional H_2 uptake was measured above 200 °C. From the TPR measurements it was concluded that reduction of the catalyst with H_2 at 300 °C before reaction was sufficient to obtain reduced Ru metal.

3.2 Hydrogenation of single component feed

Hydrogenation of AA in water was done at 120 ^oC over Ru/TiO_2 as shown in Table 2. At these conditions, 37.5 % of the AA was converted and two liquid products were observed: ethanol (78.3% selectivity) and ethyl acetate (1.4 % selectivity). Other products were

View Article Online
DOI: 10.1039/C7GC00367F

methane, ethane, and CO_2 with traces of C_3-C_5 hydrocarbons. Several investigations have found Ru to be the most active and selective metal for converting acetic acid into ethanol [24, 30, 31].

Hydrogenation of HA was faster than hydrogenation of AA. Hydrogenation of HA occurred at temperatures as low as 20°C, as shown in Figure 1. HA conversion increased from 11.7 % to 93.6 % as temperature increased from 20 to 70 °C. Under these conditions HA was selectively hydrogenated into 1,2-propanediol (PG-propylene glycol) with trace amounts of methane observed in the gas-phase. The PG selectivity was always above 98% under all conditions investigated.

3.3 Hydrogenation of two-component feed

Hydrogenation of two-component feeds (AA+HA, AA+FA) in water with Ru/TiO_2 catalyst were performed with product distributions as shown in Table 2 and Figures 1-2. Co-feeding AA+HA at 120 °C resulted in an acetic acid conversion of 45.5 % while HA was completely converted at these conditions. A small amount of propanol was detected among the products (below 1%), which was not observed when the compounds were feed separately. Propanol is probably formed as a secondary product by hydrodeoxygenation of PG. Complete conversion of the FA occurred when aqueous solutions of FA + AA were co-fed. CO_2 was the major product observed from FA with only small amounts of methanol formed. This suggests that the FA decomposes to CO_2 and H_2 rather than hydrogenates as the main reaction pathway.

Hydrogenation of HA with and without AA present in the feed is shown in Figure 1. Co-feeding 10 wt% AA increased the reactivity of HA. The effect of feeding AA or FA on the HA conversion is detailed more in Figure 2 which plots the HA conversion as a function of time on stream. PG was the only observed product for these expeirments. Neither of the two acids showed any reactivity at these reaction conditions. Increasing the AA concentration

View Article Online
DOI: 10.1039/C7GC00367F

increased the rate of hydrogenation of HA. Co-feeding 2 wt% FA together with HA completely shut off the HA conversion. Subsequently co-feeding 20 wt% AA only partly restored the HA conversion activity of the Ru-catalyst before a decreasing activity with time on stream (TOS) was observed.

In elucidating the enhancing effect of AA on the HA reactivity a reaction mechanism involving acid catalyzed enolization of HA into its enol- and enediol-form is proposed as shown in Scheme 1. Enolization is a proton transfer reaction catalyzed by acids where the rate is dependent on the acid strength (pK) and concentration [32]. Yaylayan et al. have studied the enolization reactions of HA in different solvents with FTIR spectroscopy [33]. They found no evidence of enolization of HA in D_2O, while under acidic conditions the enol and predominantly enediol tautomers were observed. The concentration of enolized species was found to increase with temperature. In addition to the route involving direction hydrogenation of the C=O bond in HA (Path 1) another parallel route opens when acid species are introduced in the feed (Path 2). In Path 2 the enediol is formed as an intermediate before rapid hydrogenation of the C=C bond takes place forming PG. The observation that the total conversion of HA increases with AA concentration implies that formation of enediol is the rate-determining step along path 2. FA should also catalyze the enolization reaction [32, 33]. The reason for the observed negative effect is believed to be a strong deactivation of the active Ru sites caused by adsorbates originating from FA. CO formation from FA decomposition has been shown experimentally to take place on Ru [34]. If CO is formed then Ru particle size becomes an important factor. Fischer-Tropsch Synthesis was found to be a highly structure-sensitive reaction on Ru clusters smaller than 10 nm [35]. Lower intrinsic activity, measured as a decreased turnover frequency of CO consumption, was found on Ru clusters less than 10 nm. This observation was related to stronger CO adsorption and concomitant blocking of active sites. The small metal clusters on the Ru/TiO_2 (Table 1) are

View Article Online
DOI: 10.1039/C7GC00367F

thus susceptible to CO poisoning at these low-temperature conditions. After removing FA from the feed a full recovery of the catalytic activity is not observed suggesting a continuing partial CO poisoning of the active sites.

3.4 Hydrogenation of three-component feed

The effect of temperature on the hydrogenation of a three-component feed, consisting of AA, HA and FA, is shown in Table 2 and Figure 3. The conversion of AA increased from 3 % to 60 % when the temperature was increased from 100 to 150 °C. The apparent activation energy (E_{app}) for AA conversion was 46.2 kJ/mol. This is comparable to the activation energy of 40.0 kJ/mol reported by Olcay et al. for the hydrogenation of AA on Ru/C in a continuous packed-bed reactor [31]. HA and FA showed similar conversion at 100 °C (64 % and 66 % respectively), while both were completely converted at 120 °C. The selectivity into liquid products was 96 % at 100 °C, decreasing to 67 % at 150 °C with a corresponding increase in the gas products. The dominant liquid product at low temperature (100 ° C) was PG (95 %). Minor liquid products (< 1 %) at 100 °C were ethanol, methanol, propanol, and ethyl acetate. When the reactor temperature increased to 150 °C PG liquid selectivity decreased to 32 %. Ethanol selectivity initially increased to 20 % at 120 °C before decreasing to 18 % at 150 °C. In the same temperature interval propanol selectivity increased from 0.1 % to 1.8 %, while methanol selectivity decreased from 0.5 % to below 0.1 %. Ethyl acetate selectivity increased to 0.4 % at 120 °C but did not increase further as temperature increased to 150 °C. Methane, CO_2, ethane, and propane were the main gas-products formed with small amounts of C_4-C_6 also observed. The selectivity to gas-phase products increased with temperature from 0.3 % at 100 °C to 38.2% at 150 °C. A reactor temperature of 150 °C resulted in pressure buildup and visual evidence of carbonaceous material on the catalyst and reactor internals. At

View Article Online
DOI: 10.1039/C7GC00367F

temperatures below 120 °C catalyst activity was stable for more than 50 hours TOS with no signs of coke formation when pumping the multi-component feed.

3.5 Hydrogenation of AFBO

The APBO was hydrogenated with Ru/C at 120 °C and 5.18 MPa pressure as shown in Table S1. Hydroxymethylfurfural (HMF), furfural, acetaldehyde, and phenol were completely converted at the shortest TOS (6 hours). Products from these reactants were HMF alcohol, furfuryl alcohol, ethanol, and cyclohexanol, respectively. High conversions of hydroxyacetaldehyde, FA, propionic acid, butyric acid, and HA were also obtained after 6 hours TOS while only partial conversion of AA took place. Products after hydrogenation were mono-alcohols: methanol > ethanol > hexanol > propanol > butanol, and diols: ethylene glycol > PG > 1,4-butanediol > 1,4-pentanediol > 2,3-butanediol > 1,5-pentanediol > 1,3-butanediol. Main gas phase products were methane and CO_2 with small amounts of higher hydrocarbons (C_2-C_6). The composition of the products decreased and the reactants increased after 25 hrs of TOS compared to the 6 h TOS point. The most significant changed was observed for AA, propionic acid, butyric acid, and HA. Hydrogenation of FA, hydroxyaldehyde, HMF, furfural, and phenol were affected the least.

Hydrogenation of AFBO was studied more in depth using Ru/TiO_2 catalyst in the temperature range of 100 °C to 140 °C at 6.21 MPa pressure, as shown in Table 3. Experiments were run for at least 8 hours at each set of operating conditions before liquid products were collected for analysis. GC-MS analysis of the liquid samples made quantification of a wider range of the compounds possible compared to the experiments with Ru/C. Feed compounds detected by GC-MS but not quantified included phenol, 2-methoxyphenol, 2,3-butanedione, 3-methyl-1,2-cyclopentadione, and 3-methyl-2-furanone. Several compounds found in the feed were completely converted even at 100 °C. These included acetone, acetaldehyde,

View Article Online
DOI: 10.1039/C7GC00367F

propionaldehyde, 2-propen-1-ol, 1-hydroxy-2-butanone, 3-hydroxy-2-butanone, 2-hexanone, and 2-furanone. Feed compounds including HMF, furfural, FA, hydroxyacetaldehyde, and HA were less reactive, requiring a reaction temperature of 140 °C to reach near complete conversion. The least reactive compounds in the bio-oil were organic acids including AA and propionic acid. The amount of butyric acid in the product decreased by 65 % relative to the feed at 140 °C, while the amount of AA decreased by 30 % with increasing temperature up to 120 °C. The AA amount in the product then increased again when the temperature was set to 140 °C. The refractory behavior of AA under LTH of bio oil with Ru/C has been documented by Elliot and Oasmaa [36, 37]. They reported only limited conversion at 150 °C after 4 h in a batch reactor with ethanol as the main product. In their work higher temperatures resulted in decreasing ethanol yield and an increase in methane production. Propionic acid content decreased initially at a reactor temperature of 100 °C, but increased at higher temperatures. 2-butanone found in the feed was stable up to 120 °C before being partially converted when the reactor temperature increased to 140 °C. Methanol and methyl acetate were present in the bio-oil feed but, unlike the other feed compounds, their concentration increased in the hydrogenated product.

Table 3 also lists the product distribution. The most abundant liquid products were methanol > PG >ethylene glycol > 1,4-butanediol > 1,4-pentanediol > 1,2-butanediol and 2,3-butanediol. Other products formed in minor amounts were ethanol, n-propanol, n-butanols, cyclopentanol, 1,2-butanol, butyrolactone, and furfuryl alcohol, and 1-hexanol. A small amount of ethyl acetate was also observed. A pronounced effect of reaction temperature on the product distribution was observed. Methanol concentration was highest at 100 °C before decreasing at higher temperatures. The same behavior was observed with 1,2-ethanediol and 1,4-butanediol (above 120 °C). Sanna et al. reported similar shifts in product selectivity for

View Article Online
DOI: 10.1039/C7GC00367F

HDO of the water soluble fraction of bio-oil over Ru/C catalyst [38]. Sanna et al. observed that the HA concentration decreases and the AA, furufral and phenolic concentrations did not change when no catalyst was present in the reactor. Selectivity to gas-phase products was below 10% in the investigated temperature range with the most abundant products being methane and CO_2.

An interesting question is how close the product yields of these mono-alcohols and diols are to the potential product yields that can be obtained for a given feed composition. Table 4 summarize the theoretical potential yields of different alcohols assuming complete and selective conversion of the listed feed molecules into conceivable products. A product yield exceeding the theoretical yield indicates that the product molecule is formed in parallel reactions originating from additional feed compounds or intermediate products. Ethanol was only formed in yields lower than 3% of the theoretical yield throughout the entire investigated reaction temperature window. The listed butanediols and 1,4-pentanediol were produced in high yields close to and above the theoretical values at the operating conditions. The yield of PG increased from 6% of the theoretical yield at 100 °C to 90% at 140 °C. In contrast to other diols, ethylene glycol yield decreased with temperature, going from 36% at 100 °C to 5% at 140 °C.

In summary, the main reactions occurring during hydrogenation of light oxygenates in AFBO included conversion of hydroxy-ketones into diols and hydrogenation of ketones and aldehydes into mono-alcohols. HDO of carboxylic acids to produce mono-alcohols proceeded with low selectivity. The resulting decrease in carbonyl content after hydrogenation improved stability of the bio-oil, which might be a useful pretreatment ahead of further upgrading.

3.6 Comparison of model-feed to aqueous fraction bio-oil processing

View Article Online
DOI: 10.1039/C7GC00367F

The reactivity of model compounds is compared to that of AFBO in Table 5. AA was the least reactive compound with FA being the most reactive one. Complete conversions of FA and HA were obtained at most of the reaction conditions when studying two- and three-component model feeds. The complex composition of the AFBO also induces differences in the observed product selectivity. There was a striking difference in the reactions for AA between the model and real feeds. Ethanol was the dominant product from AA with selectivity above 60% in the model feeds. In the AFBO the ethanol selectivity from AA hydrogenation was 6% and 26% on Ru/TiO_2 and Ru/C respectively. This is based on the assumption that the produced ethanol originates from AA hydrogenation. The reaction network for aqueous phase hydrogenation of AA on Ru proposed by Wan [24] and Olcay [30] involves formation of acetyl species followed by ethanol formation via acetaldehyde when hydrogen is present. Our experimental data indicates that this reaction path is suppressed in AFBO and that an equally important source of ethanol is the direct hydrogenation of acetaldehyde originally present in the feed. The question then is what other chemical reactions are contributing in the transformation of AA. Esterification of AA with methanol forming methyl acetate seems to be responsible for the increased amount of this compound in the product. Formation of methyl acetate during bio-oil upgrading under hydrogen pressure and with a Ru/Al_2O_3 catalyst was also reported by Ying et al. [39]. As stated earlier esterification of AA with ethanol producing ethyl acetate only take place to a limited degree.

Methanol formation was catalyzed by both Ru/TiO_2 and Ru/C during the hydrogenation of APBO. Scheme 2 shows reaction pathways suggesting how methanol can be formed from hydroxyacetaldehyde over the Ru catalysts. Hydroxyacetaldehyde is first hydrogenated into ethylene glycol (reaction pathway I) followed by cleavage of the C-C bond and formation of methanol as a secondary product. Direct cleavage of the C-C bond in hydroxyacetaldedyde with formation of methanol and formaldehyde products (reaction pathway II) is also

View Article Online
DOI: 10.1039/C7GC00367F

suggested but no formaldehyde was detected among the products. Several investigations of aqueous phase hydrogenation of hydroxyacetaldehyde have found ethylene glycol as the sole product [14, 40, 41]. The less than stoichiometric amount of ethylene glycol produced compared to the amount of converted hydroxyacetaldehyde (Table S1 and 3) found in the present study shows that ethylene glycol reacts further at the employed reaction conditions. These earlier studies were conducted at lower temperatures (75-90°C). High C-C bond cleavage activity of Ru has been reported for ethylene glycol aqueous phase reforming conducted at higher temperatures [15]. Chemical composition analysis of the studied AFBO showed the presence of levoglucosan as a feed molecule [9]. Levoglucosan can be converted into sorbitol which could then undergo further hydrogenolysis into C_2-C_4 diols and mono-alcohols [38].

3.7 Catalyst Stability

The AA, FA and HA conversion decreased with time when processing AFBO, as shown in Figure 4. From 21 to 106 hours TOS the conversion of AA decreased from 30% to 1% (97% reduction). FA conversion decreased from 80% to 27% (66% reduction), and HA conversion from 40% to 6% (85% reduction). Characterization of the catalysts after processing APBO were performed (Table 1). Chemisorption measurements on the catalysts after reaction resulted in decreased H_2 uptake for both catalysts. The H_2 uptake on the used Ru/C catalyst was reduced by 89% while the corresponding reduction on the Ru/TiO_2 catalyst was 63%. The BET surface area was reduced by 81% and 5% on the used Ru/C and Ru/TiO_2, respectively. The effect of reaction conditions on catalyst pore volume was much more pronounced for Ru/C compared to Ru/TiO_2 with a reduction of 59% compared to 5%. The high surface area carbon support contains pores of considerably smaller size compared to the TiO_2 support. The observed increase in average pore size after reaction is a consequence of catalyst fouling due to carbonaceous deposits.

View Article Online
DOI: 10.1039/C7GC00367F

There was a notable effect of temperature on Ru/TiO_2 catalyst stability. When processing model-feeds, gas-make increased sharply with temperature. Pressure drop increased across the reactor when running the reactions at 150 °C, Within a few hours of operation the reactor plugged due to coke formation. The observed decline in catalyst activity at lower temperatures is probably not attributed to coke buildup on the catalyst surface alone. A contributing factor seems to be acid leaching of ruthenium metal from the catalyst caused by the low pH of the feeds. ICP measurements of the liquid products from the multi-component feed (AA+HA+FA) for the Ru/TiO_2 catalyst detected Ru with highest concentration (110 ppm) at short TOS (24 h) decreasing to 30 ppm after 68 h TOS. Based on an average leaching rate, this amounts to roughly 25 % of the Ru being leached out of solution during the experiment. This substantial loss of Ru is expected to influence catalyst performance during 90 hours TOS.

Biomass contains trace amounts of elements like potassium, phosphorus, chlorine, and sulfur, which will appear in the products of fast pyrolysis [1]. Analysis of wood-derived char and bio-oil shows that most of the ash-forming elements are retained in the char (above 90%) while much of the sulfur and chlorine can be found in the bio-oil [42, 43, 44]. Based on elemental analysis of the AFBO used in our study [9] a concentration of approximately 68 ppm in the feed was previously measured. Sulfur species adsorb strongly on most metals creating stable surface sulfides [45]. This modifies the adsorption characteristics of other molecules by blocking chemisorption sites. Lowering of the H_2-adsorption capacity and decreased hydrogen binding energy take place on presulfided metal surfaces. Catalyst deactivation by sulfur poisoning was found to be significant during low temperature hydrogenation of bio-oil over a Ru/TiO_2 catalyst [46]. The bio-oil contained 68 ppm sulfur as reported elsewhere [9]. Lowered hydrogenation activity resulted in increased catalyst fouling by carbonaceous species. Reducing the sulfur content in the bio-oil feed to 39 ppm resulted in

View Article Online
DOI: 10.1039/C7GC00367F

higher hydrogen-to-carbon ratio and lower carbonyl concentration in the hydrogenated product. Our results supports the role of sulfur acting as a poison affecting the hydrogenation function of the catalysts. Decreasing conversion with TOS and significant reduction in H_2 uptake on the used catalysts from blocking of active Ru sites by sulfur and carbonaceous species are observed. The latter being most detrimental on the carbon-support due to its smaller pores. Declining catalyst activity when processing the aqueous phase bio-oil could also be due in part to CO poisoning of the catalyst surface from formic acid decomposition. The observed shift in Table 3 from CH_4 and CO_2 being dominant to CO indicates declines in water-gas-shift (WGS) and methanization reactions with time.

4. Conclusions

We have performed experiments on hydrogenation over Ru catalysts of single- and multi-component model compounds and the aqueous fraction of bio-oil collected through staged recovery of pyrolysis vapors. The order of increasing rate of hydrogenation is the same whether processing single- or multi-component model compounds or APBO with the rate decreasing as: formic acid> hydroxyacetone > acetic acid. When present in the model feeds formic acid undergoes dehydrogenation as the main reaction route forming CO_2 and H_2. The product selectivity to methanol is below 1 %. Hydrogenation of hydroxyacetone gives propylene glycol as the dominant product. Hydrogenation of acetic acid produces ethanol at high selectivity with ethyl acetate as a minor product.

Co-feeding acetic acid and hydroxyacetone increase the hydrogenation rate of hydroxyacetone. A mechanism involving the acid-catalyzed enolization of hydroxyacetone into its enol-form (prop-2-ene-1,2-diol) is proposed. The observation that the total conversion of hydroxyacetone increases with acetic acid concentration implies that formation of the

View Article Online
DOI: 10.1039/C7GC00367F

intermediate enol is the rate-determining step. Co-feeding 2 wt% formic acid together with hydroxyacetone completely shuts off hydroxyacetone conversion.

The main reactions occurring during hydrogenation of the light oxygenates in AFBO include conversion of hydroxy-ketones into diols and hydrogenation of ketones and aldehydes into mono-alcohols. HDO of carboxylic acids into corresponding mono-alcohols proceeds with low selectivity. The resulting decrease in carbonyl content after hydrogenation contribute towards stabilizing the bio-oil if performed as an intermediate step before further processing either alone or in combined streams in an integrated chemical facility.

This study shows differences in product selectivity for AA when present as single- and multi-compound in water or in AFBO. High selectivity to ethanol is found when model-feed mixtures containing AA are hydrogenated. This is in contrast to APBO hydroprocessing where the ethanol selectivity (at comparable AA conversion) is low.

Catalyst activity and stability were influenced by several factors. Higher temperature (~150 °C) resulted in catalyst fouling from carbon deposition. Reduction in BET surface area and pore volume with reaction time was found to be more pronounced for Ru/C catalyst compared to Ru/TiO_2. Loss of Ru from the catalyst as a result of acid leaching was observed. Ru metal content on the catalyst was observed to decrease by about 25 % after 90 hours on stream. An increased rate of catalyst deactivation was observed during hydrogenation of AFBO compared to model-feed mixtures. Catalyst poisoning by sulfur present in the AFBO is suggested to be an important factor.

View Article Online
DOI: 10.1039/C7GC00367F

Acknowledgment

We appreciate the support of Lysle Whitmer, Marge Rover, and Ryan Smith at Iowa State University who prepared and analyzed the bio-oil samples used in these experiments.

1. Huber, G.W., S. Iborra, and A. Corma, *Synthesis of transportation fuels from biomass: Chemistry, catalysts, and engineering.* Chemical Reviews, 2006. **106**(9): p. 4044-4098.
2. Bridgwater, A.V., *Review of fast pyrolysis of biomass and product upgrading.* Biomass and Bioenergy, 2012. **38**(0): p. 68-94.
3. Mohan, D., C.U. Pittman Jr, and P.H. Steele, *Pyrolysis of wood/biomass for bio-oil: A critical review.* Energy and Fuels, 2006. **20**(3): p. 848-889.
4. Czernik, S. and A.V. Bridgwater, *Overview of applications of biomass fast pyrolysis oil.* Energy and Fuels, 2004. **18**(2): p. 590-598.
5. Oasmaa, A. and E. Kuoppala, *Fast pyrolysis of forestry residue. 3. Storage stability of liquid fuel.* Energy and Fuels, 2003. **17**(4): p. 1075-1084.
6. Chen, W., et al., *Low temperature hydrogenation of pyrolytic lignin over Ru/TiO2: 2D HSQC and 13C NMR study of reactants and products.* Green Chemistry, 2016. **18**(1): p. 271-281.
7. Elliott, D.C. and E.G. Baker, *Process for upgrading biomass pyrolyzates*. 1989: USA.
8. Brown, R.C. and T.R. Brown, *Thermochemical Processing of Lignocellulosic Biomass*, in *Biorenewable Resources*. 2014, John Wiley & Sons, Inc. p. 195-236.
9. Pollard, A.S., M.R. Rover, and R.C. Brown, *Characterization of bio-oil recovered as stage fractions with unique chemical and physical properties.* Journal of Analytical and Applied Pyrolysis, 2012. **93**(0): p. 129-138.
10. Rover, M.R., et al., *The effect of pyrolysis temperature on recovery of bio-oil as distinctive stage fractions.* Journal of Analytical and Applied Pyrolysis, 2014. **105**(0): p. 262-268.
11. Resasco, D.E. and S.P. Crossley, *Implementation of concepts derived from model compound studies in the separation and conversion of bio-oil to fuel.* Catalysis Today, 2015. **257**(P2): p. 185-199.
12. Pham, T.N., D. Shi, and D.E. Resasco, *Evaluating strategies for catalytic upgrading of pyrolysis oil in liquid phase.* Applied Catalysis B: Environmental, 2014. **145**: p. 10-23.
13. Nie, L. and D.E. Resasco, *Improving carbon retention in biomass conversion by alkylation of phenolics with small oxygenates.* Applied Catalysis A: General, 2012. **447-448**: p. 14-21.
14. Vispute, T.P. and G.W. Huber, *Production of hydrogen, alkanes and polyols by aqueous phase processing of wood-derived pyrolysis oils.* Green Chemistry, 2009. **11**(9): p. 1433-1445.
15. Davda, R.R., et al., *A review of catalytic issues and process conditions for renewable hydrogen and alkanes by aqueous-phase reforming of oxygenated hydrocarbons over supported metal catalysts.* Applied Catalysis B: Environmental, 2005. **56**(1-2 SPEC. ISS.): p. 171-186.
16. Bond, J.Q., et al., *Production of renewable jet fuel range alkanes and commodity chemicals from integrated catalytic processing of biomass.* Energy & Environmental Science, 2014. **7**(4): p. 1500-1523.
17. Furimsky, E., *Catalytic hydrodeoxygenation.* Applied Catalysis A: General, 2000. **199**(2): p. 147-190.
18. Elliott, D.C., *Historical Developments in Hydroprocessing Bio-oils.* Energy & Fuels, 2007. **21**(3): p. 1792-1815.
19. Mortensen, P.M., et al., *A review of catalytic upgrading of bio-oil to engine fuels.* Applied Catalysis A: General, 2011. **407**(1–2): p. 1-19.

View Article Online
DOI: 10.1039/C7GC00367F

20. Lødeng, R., et al., *Chapter 11 - Catalytic Hydrotreatment of Bio-Oils for High-Quality Fuel Production*, in *The Role of Catalysis for the Sustainable Production of Bio-fuels and Bio-chemicals*, K.S.T.A.L. Stöcker, Editor. 2013, Elsevier: Amsterdam. p. 351-396.
21. Boullosa-Eiras, S., et al., *Chapter 2 Potential for metal-carbide, -nitride, and -phosphide as future hydrotreating (HT) catalysts for processing of bio-oils*, in *Catalysis: Volume 26*. 2014, The Royal Society of Chemistry. p. 29-71.
22. Chen, L., et al., *Aqueous-phase hydrodeoxygenation of carboxylic acids to alcohols or alkanes over supported Ru catalysts.* Journal of Molecular Catalysis A: Chemical, 2011. **351**(0): p. 217-227.
23. Luo, W., et al., *Ruthenium-catalyzed hydrogenation of levulinic acid: Influence of the support and solvent on catalyst selectivity and stability.* Journal of Catalysis, 2013. **301**(0): p. 175-186.
24. Wan, H., R.V. Chaudhari, and B. Subramaniam, *Aqueous phase hydrogenation of acetic acid and its promotional effect on p-cresol hydrodeoxygenation.* Energy and Fuels, 2013. **27**(1): p. 487-493.
25. Wan, H., et al., *Kinetic investigations of unusual solvent effects during Ru/C catalyzed hydrogenation of model oxygenates.* Journal of Catalysis, 2014. **309**(0): p. 174-184.
26. Newman, C., et al., *Effects of support identity and metal dispersion in supported ruthenium hydrodeoxygenation catalysts.* Applied Catalysis A: General, 2014. **477**(0): p. 64-74.
27. Wildschut, J., et al., *Hydrotreatment of fast pyrolysis oil using heterogeneous noble-metal catalysts.* Industrial and Engineering Chemistry Research, 2009. **48**(23): p. 10324-10334.
28. Wildschut, J., et al., *Insights in the hydrotreatment of fast pyrolysis oil using a ruthenium on carbon catalyst.* Energy and Environmental Science, 2010. **3**(7): p. 962-970.
29. Taylor, K.C., *Determination of ruthenium surface areas by hydrogen and oxygen chemisorption.* Journal of Catalysis, 1975. **38**(1–3): p. 299-306.
30. Olcay, H., et al., *Aqueous-phase hydrogenation of acetic acid over transition metal catalysts.* ChemCatChem, 2010. **2**(11): p. 1420-1424.
31. Olcay, H., Y. Xu, and G.W. Huber, *Effects of hydrogen and water on the activity and selectivity of acetic acid hydrogenation on ruthenium.* Green Chemistry, 2014. **16**(2): p. 911-924.
32. Lienhard, G.E. and T.C. Wang, *On the mechanism of acid-catalyzed enolization of ketones.* Journal of the American Chemical Society, 1969. **91**(5): p. 1146-1153.
33. Yaylayan, V.A., S. Harty-Majors, and A.A. Ismail, *Monitoring carbonyl-amine reactions and enolization of 1-hydroxy-2-propanone (acetol) by FTIR spectroscopy.* Journal of Agricultural and Food Chemistry, 1999. **47**(6): p. 2335-2340.
34. Sun, Y.K., and W.H. Weinberg, *Catalytic decomposition of formic acid on Ru(001): Transient measurements.* Journal of Chemical Physics, 1991. **94**: p. 4587-4599.
35. Gonzalez Carballo, J.M., Y. Jang, A. Holmen, S. Garcia-Rodriguez, S. Rojas, M. Ojeda, and J.L.G. Fierro, *Catalytic effects of ruthenium particle size on the Fischer-Tropsch Synthesis.* Journal of Catalysis, 2011. **284**: p. 102-108.
36. Elliott, D.C. and T.R. Hart, *Catalytic hydroprocessing of chemical models for bio-oil.* Energy and Fuels, 2009. **23**(2): p. 631-637.
37. Oasmaa, A., et al., *Characterization of Hydrotreated Fast Pyrolysis Liquids.* Energy & Fuels, 2010. **24**(9): p. 5264-5272.
38. Sanna, A., T.P. Vispute, and G.W. Huber, *Hydrodeoxygenation of the aqueous fraction of bio-oil with Ru/C and Pt/C catalysts.* Applied Catalysis B: Environmental, 2015. **165**: p. 446-456.
39. Ying, X., et al., *Upgrading of fast pyrolysis liquid fuel from biomass over Ru/γ-Al2O3 catalyst.* Energy Conversion and Management, 2012. **55**: p. 172-177.
40. Mahfud, F.H., F. Ghijsen, and H.J. Heeres, *Hydrogenation of fast pyrolyis oil and model compounds in a two-phase aqueous organic system using homogeneous ruthenium catalysts.* Journal of Molecular Catalysis A: Chemical, 2007. **264**(1–2): p. 227-236.
41. Bindwal, A.B., A.H. Bari, and P.D. Vaidya, *Kinetics of low temperature aqueous-phase hydrogenation of model bio-oil compounds.* Chemical Engineering Journal, 2012. **207-208**: p. 725-733.

View Article Online
DOI: 10.1039/C7GC00367F

42. Trinh, T.N., et al., *Comparison of lignin, macroalgae, wood, and straw fast pyrolysis.* Energy and Fuels, 2013. **27**(3): p. 1399-1409.
43. Jung, S.-H., S.-J. Kim, and J.-S. Kim, *Characteristics of products from fast pyrolysis of fractions of waste square timber and ordinary plywood using a fluidized bed reactor.* Bioresource Technology, 2012. **114**(0): p. 670-676.
44. Leijenhorst, E.J., W. Wolters, L. van de Beld, and W. Prins, *Inorganic element transfer from biomass to fast pyrolysis oil: Review and experimentsr.* Fuel Processing Technology, 2016. **149**: p. 96-111.
45. Bartholomew, C.H., P.K. Agrawal, and J.R. Katzer, *Sulfur poisoning of metals.* Adv. Catal., 1982. **31**: p. 135-242.
46. Wang, H., S.-J. Lee, M.V. Olarte, and A.H. Zacher, *Bio-oil stabilization by hydrogenation over reduced metal catalysts at low temperature.* ACS Sustainable Che.m Eng., 2016. **4**: p. 5533-5545.

View Article Online
DOI: 10.1039/C7GC00367F

Table 1 Metal loading, H_2 uptake, metal dispersion analysis, surface average metal particle size, BET surface area, pore volume and average pore size of Ruthenium catalysts.

Property	Ru/C fresh	Ru/C used[a]	Ru/TiO_2 fresh	Ru/TiO_2 used[a]
metal loading (wt%)	5	-	3	-
H_2 uptake (μmol/g)	38.5	4.2	193.2	70.7
metal dispersion (%)	7.8	-	65.1	-
metal particle size (nm)	11.7	-	1.4	-
BET surface area (m^2/g)	834	162	57	54
pore volume (cm^3/g)	0.80	0.33	0.31	0.27
average pore size (Å)	38.4	81.4	214.7	196.5

[a] Characterization of catalyst after reaction with AFBO.

Table 2 Hydrogenation of model compounds in aqueous phase over 3 wt% Ru/TiO_2 catalyst. (AA) acetic acid, (HA) hydroxyacetone, (FA) formic acid. Reaction conditions: 6.21 MPa, H_2 flow rate 40 mL min^{-1}.

Feedstock	AA	HA	AA+HA	AA+FA	AA+HA+FA	AA+HA+FA	AA+HA+FA	AA+HA+FA
Time on stream (h)	33	14	11	22	11	79	11	45
Reaction temperature, °C	120	70	120	120	120	100	120	150
WHSV, h^{-1}	1.5	20	1.5	1.5	1.5	0.75	0.75	0.75
Acetic acid conversion, %	37.5	-	45.5	33.4	19.2	3.0	40.8	60.4
Hydroxyacetone conversion, %	-	93.6	100.0	-	100.0	63.5	100.0	99.8
Formic acid conversion, %	-	-	-	100.0	100.0	65.7	100.0	100
Carbon in gas effluent, %	7.1	0.1	5.9	10.2	8.9	0.3	13.9	38.2
Carbon in liquid effluent, %	91.1	97.1	96.2	79.1	96.6	95.6	84.9	67.2
Carbon balance, %	98.2	97.2	102.1	89.3	105.5	95.9	98.8	105.4
Carbon selectivity, %								
CO_2	5.0	0	2.3	9.6	5.0	0.0	6.6	14.2
Methane	8.3	0.1	3.7	16.0	7.8	1.0	10.4	22.2
Ethane	6.5	0	2.6	6.9	2.0	0.3	4.0	8.2
Propane	0.1	0	0.3	1.1	0.7	0.1	0.9	2.4
Butane	0.1	0	0	0.4	0.5	0.0	0.4	0.4
Pentane	0.1	0	0.1	0.2	0.3	2.3	0.3	0.3
Hexane	0	0	0	0.1	0.2	0.0	0.2	0.2
Methanol	0	0	0	0.3	0.2	0.5	0.1	0.0
Ethanol	78.3	0	30.4	64.0	13.1	0.6	20.1	17.9
Propanol	0	0	0.9	0.1	0.4	0.1	0.7	1.8
1,2-propanediol	0	99.9	58.9	0	69.4	94.7	56.1	31.9
Ethyl acetate	1.4	0	0.5	1.0	0.4	0.1	0.4	0.4

View Article Online
DOI: 10.1039/C7GC00367F

Table 3 Aqueous phase hydrogenation of the light oxygenate fraction of bio oil over 3 wt% Ru/TiO_2 catalyst. Reaction conditions: Pressure 6.21 MPa and H_2 flow rate 40 mL min^{-1}. (n.d.: not detected).

Temperature (°C)		100	120	140	120	120	120
WHSV (h^{-1})		1.5	1.5	1.5	0.75	0.5	1.5
Species (mmol L^{-1})	Feed	9h	21h	31h	68h	93h	106h
Acetic acid	1936.6	1416.3	1355.0	1675.1	1718.2	1706.5	1913.8
Hydroxymethylfurfural	0.9	0.5	0.3	n.d.	0.3	0.3	0.6
Furfural	61.6	3.2	n.d.	n.d.	0.6	0.6	2.2
Formic acid	230.8	120.1	45.1	2.0	117.0	121.7	169.1
Acetone	12.4	n.d.	n.d.	n.d.	n.d.	n.d.	n.d.
Acetaldehyde	28.7	n.d.	n.d.	n.d.	n.d.	n.d.	4.6
Methyl acetate	85.6	115.7	95.5	107.4	137.8	156.8	96.7
Propionaldehyde	4.6	n.d.	n.d.	n.d.	n.d.	n.d.	1.2
2-propen-1-ol	15.1	n.d.	n.d.	n.d.	n.d.	n.d.	n.d.
2-butanone	3.9	3.6	3.7	1.6	6.7	7.4	5.7
1-OH-2-butanone	25.8	n.d.	n.d.	n.d.	n.d.	n.d.	n.d.
3-OH-2-butanone	21.4	n.d.	n.d.	n.d.	n.d.	n.d.	n.d.
2-hexanone	3.0	n.d.	n.d.	n.d.	n.d.	n.d.	n.d.
3-hexanone	2.9	1.5	n.d.	n.d.	n.d.	n.d.	n.d.
2-furanone	97.7	n.d.	n.d.	n.d.	n.d.	n.d.	19.8
Cyclopentanol	0.9	3.5	12.3	21.0	1.1	9.6	1.6
Methanol	423.8	823.1	591.4	495.8	522.3	470.2	505.0
Ethanol	4.1	42.8	34.8	45.5	35.0	35.8	26.7
Hydroxyacetaldehyde	610.7	28.8	12.9	n.d.	n.d.	n.d.	31.8
Hydroxyacetone	477.5	477.1	285.9	20.2	419.1	363.3	451.4
Propionic acid	104.9	78.1	113.4	133.3	122.7	124.8	112.0
Butyric acid	211.2	178.8	161.7	74.4	203.4	171.2	189.8
1-propanol		11.2	13.8	14.1	11.5	10.5	10.1
2-propanol		2.0	3.7	10.2	n.d.	n.d.	n.d.
1,2-propanediol		28.8	166.6	428.7	10.0	14.2	n.d.
Ethylene glycol		221.3	194.5	27.4	77.4	55.6	61.3
Ethyl acetate		2.0	n.d.	n.d.	1.7	1.9	0.9
1-butanol		9.8	12.7	12.2	11.2	10.8	9.0
2-butanol			2.9	8.7			
1,2-butanediol		19.5	25.0		19.7		11.9
1,4-butanediol		79.7	152.9	126.5	81.1	66.6	30.7
2,3-butanediol		13.3	31.7	108.1	29.5	31.8	14.6
Butyrolactone		17.9	18.0	10.4	18.1	16.2	15.2
1,4-pentanediol		66.4	60.0	74.5		44.4	29.9
Furfuryl alcohol		16.4	8.2				
1-hexanol		5.0	5.8	3.2		6.5	5.0
Carbon identified in liquid	9617	8348	7999	8057	7951	7778	8236
TOC in liquid	14453	12139	13438	12419	12784	12820	13311
Carbon in liquid phase (%)		84	93	86	89	89	92
Carbon in gas phase (%)		10	5	10	10	10	5
C sel. in gas phase (%)							
Methane		47	53	52	38	33	21
Ethane		4	4	5	4	3	4
C_{3-5} alkanes		19	11	11	31	33	40
CO_2		30	32	32	17	18	11
CO		0	0	0	10	13	24

Table 4 Potential and actual product yield for hydrogenation of light fraction of bio-oil over 3 wt% Ru/TiO_2 catalyst. Reaction conditions: Pressure 5.18 MPa, WHSV 1.5 h^{-1}, and H_2 flow rate 40 mL min^{-1}.

Aqueous phase feed		Potential product yield[a]		Yield (%)[b]		
Species	Wt%		wt%	100°C	120°C	140°C
Acetic acid	11.63	Ethanol	8.92	2.0	1.6	2.1
Hydroxyacetaldehyde	3.67	Ethylene Glycol	3.79	36.1	31.9	4.5
Hydroxyacetone	3.54	Propylene Glycol	3.64	6.0	34.9	89.6
2-furanone	0.82	1,4-butanediol	0.88	81.8	156.8	129.5
1-OH-2-butanone	0.23	1,2-butanediol	0.24	75.0	95.8	-
3-OH-2-butanone	0.19	2,3-butanediol	0.19	63.2	152.6	510.5
Furfural	0.59	1,4-pentanediol	0.64	107.8	96.9	121.9

a. Potential product yield = mass of feed x MW of product/MW of feed.

b. Yield = mass of product produced divided by mass of potential product yield.

View Article Online
DOI: 10.1039/C7GC00367F

Table 5 Conversion of individual compounds in model feed and the aqueous phase bio oil over the Ru catalysts. H_2 flow rate 40 mL min^{-1}.

Feedstock	AA	AA+HA	AA+FA	AA+HA+FA	Bio oil	Bio oil
Catalyst	Ru/TiO_2	Ru/TiO_2	Ru/TiO_2	Ru/TiO_2	Ru/TiO_2	Ru/C
Time on stream (h)	33	11	22	24	21	6
Reaction temperature, °C	120	120	120	120	120	120
Pressure, MPa	6.21	6.21	6.21	6.21	6.21	5.18
WHSV, h^{-1}	1.5	1.5	1.5	1.5	1.5	1.5
AA conversion, %	38	46	33	36	27	33
HA conversion, %		100		86	38	99
FA conversion, %			100	96	79	97
$S_{ethanol}$, %[1]	78	66	65	68	6	26

[1]:

$$S_{ethanol} = \frac{C_{ethanol\ in\ product} V_{outlet} - C_{ethanol\ in\ feed} V_{inlet}}{C_{acetic\ acid\ in\ feed} V_{inlet} - C_{acetic\ acid\ in\ product} V_{outlet}} * 100$$

View Article Online
DOI: 10.1039/C7GC00367F

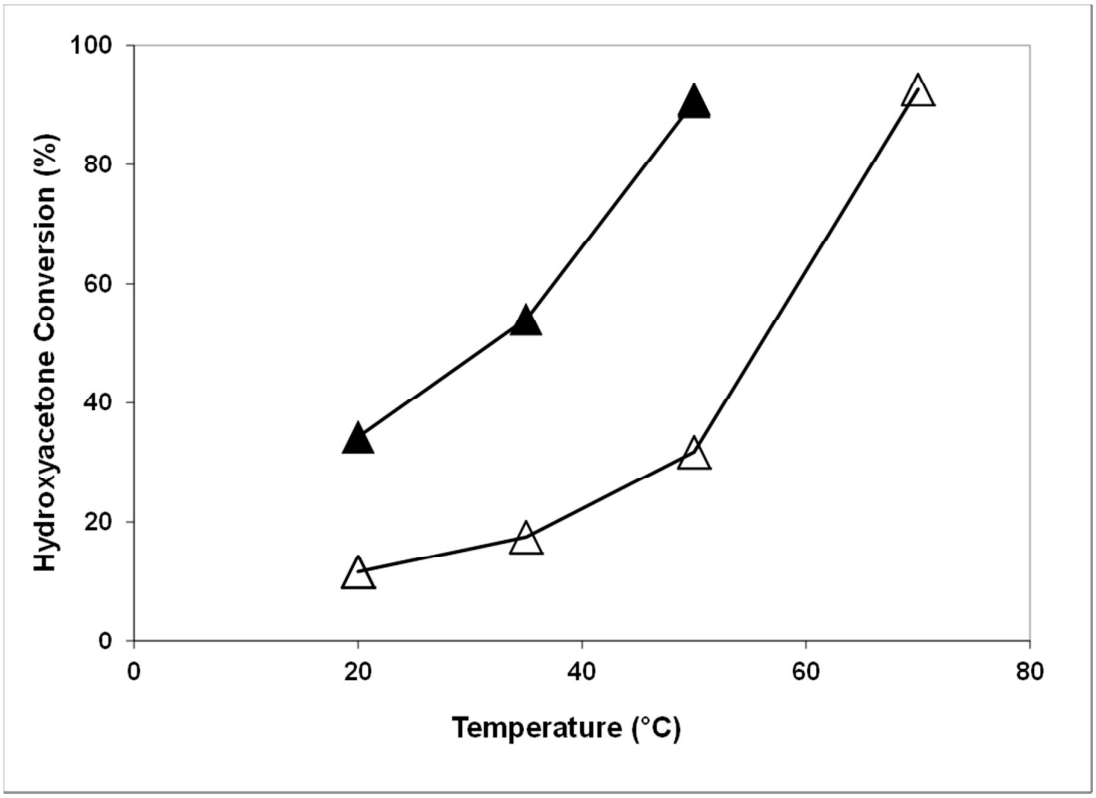

Figure 1 Hydrogenation of hydroxyacetone in aqueous phase over 3 wt% Ru/TiO_2. Reaction conditions: Pressure 6.21 MPa, WHSV 20 h^{-1}, H2 flow rate 40 mL min^{-1}. (Δ) 5 wt% hydroxyacetone, (▲) 5 wt% hydroxyacetone+10 wt% acetic acid.

View Article Online
DOI: 10.1039/C7GC00367F

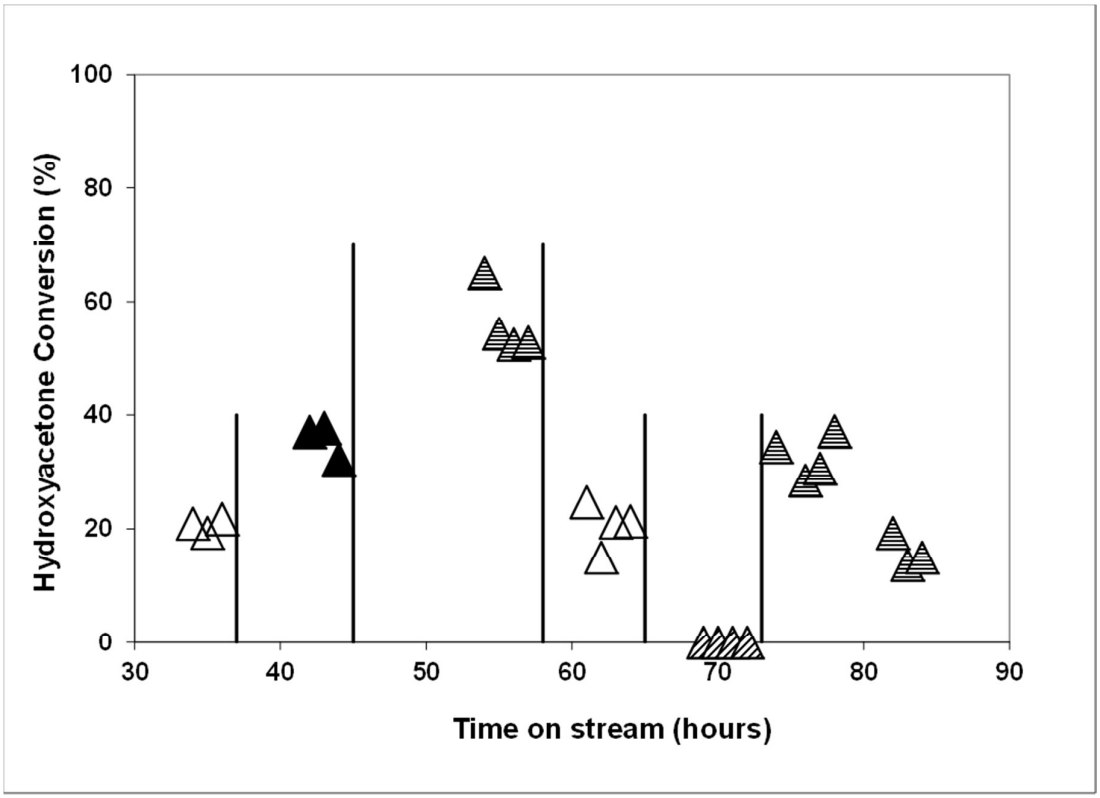

Figure 2 Effect of acetic acid and formic acid on hydrogenation of hydroxyacetone over 3 wt% Ru/TiO_2. Reaction conditions: Pressure 6.21 MPa, temperature 50 °C, WHSV 20 h^{-1}, H_2 flow rate 40 mL min^{-1}. Legend: (open triangle) 5 wt% hydroxyacetone, (black triangle) 5 wt% hydroxyacetone and 10 wt% acetic acid, (horizontally lined triangle) 5 wt% hydroxyacetone and 20 wt% acetic acid, (diagonally lined triangle) 5 wt% hydroxyacetone and 2 wt% formic acid.

View Article Online
DOI: 10.1039/C7GC00367F

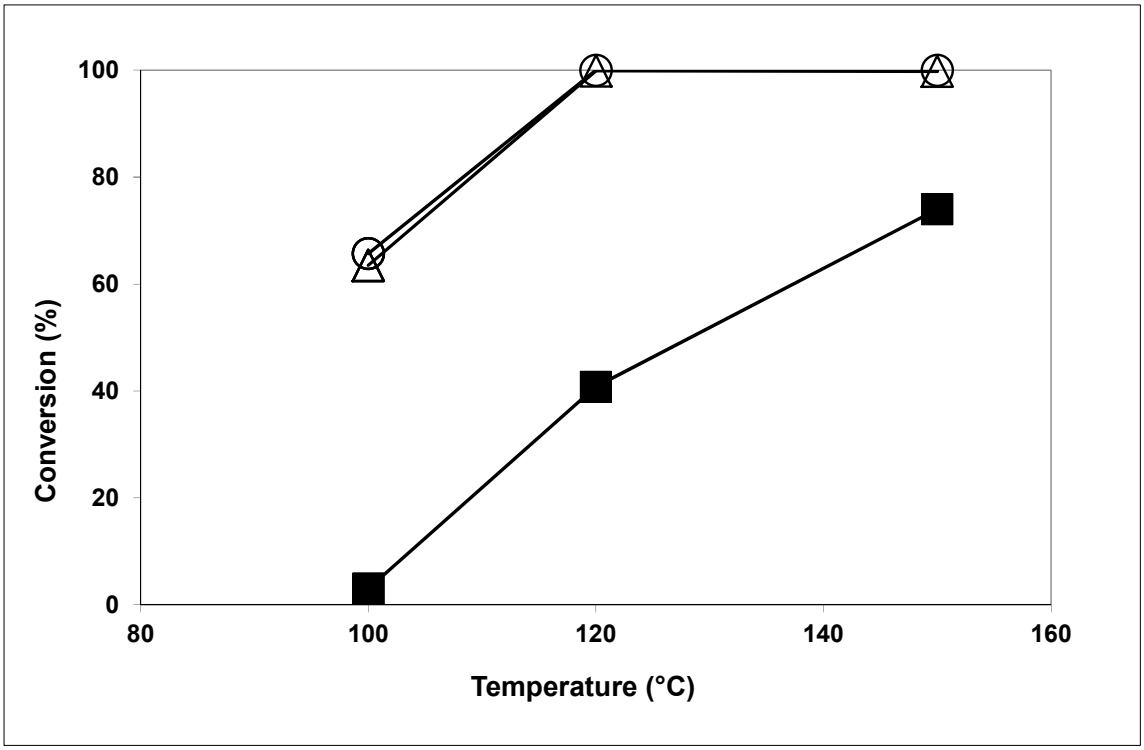

Figure 3 Effect of temperature on aqueous phase hydrogenation of three-component feed comprised of 5 wt% hydroxyacetone, 10 wt% acetic acid and 2 wt% formic acid over 3 wt% Ru/TiO_2. Reaction conditions: Pressure 6.21 MPa, WHSV 0.75 h^{-1}, H_2 flow rate 40 mL min^{-1}. Legend: (filled square) acetic acid, (open circle) formic acid, (open triangle) hydroxyacetone.

View Article Online
DOI: 10.1039/C7GC00367F

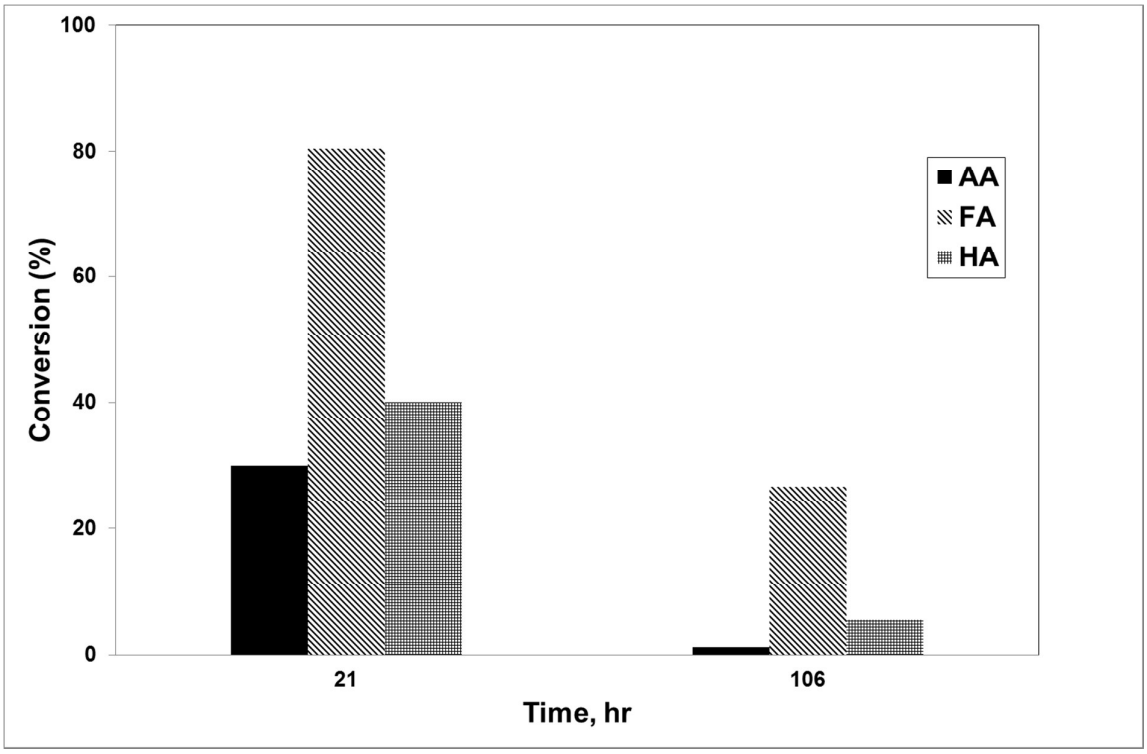

Figure 4 Conversion of acetic acid, formic acid, and hydroxyacetone in AFBO at 21 and 106 hours time-on-stream with Ru/TiO_2 catalyst. Reaction conditions: Pressure 6.21 MPa, WHSV 1.5 h^{-1}, H_2 flow rate 40 mL min^{-1}.

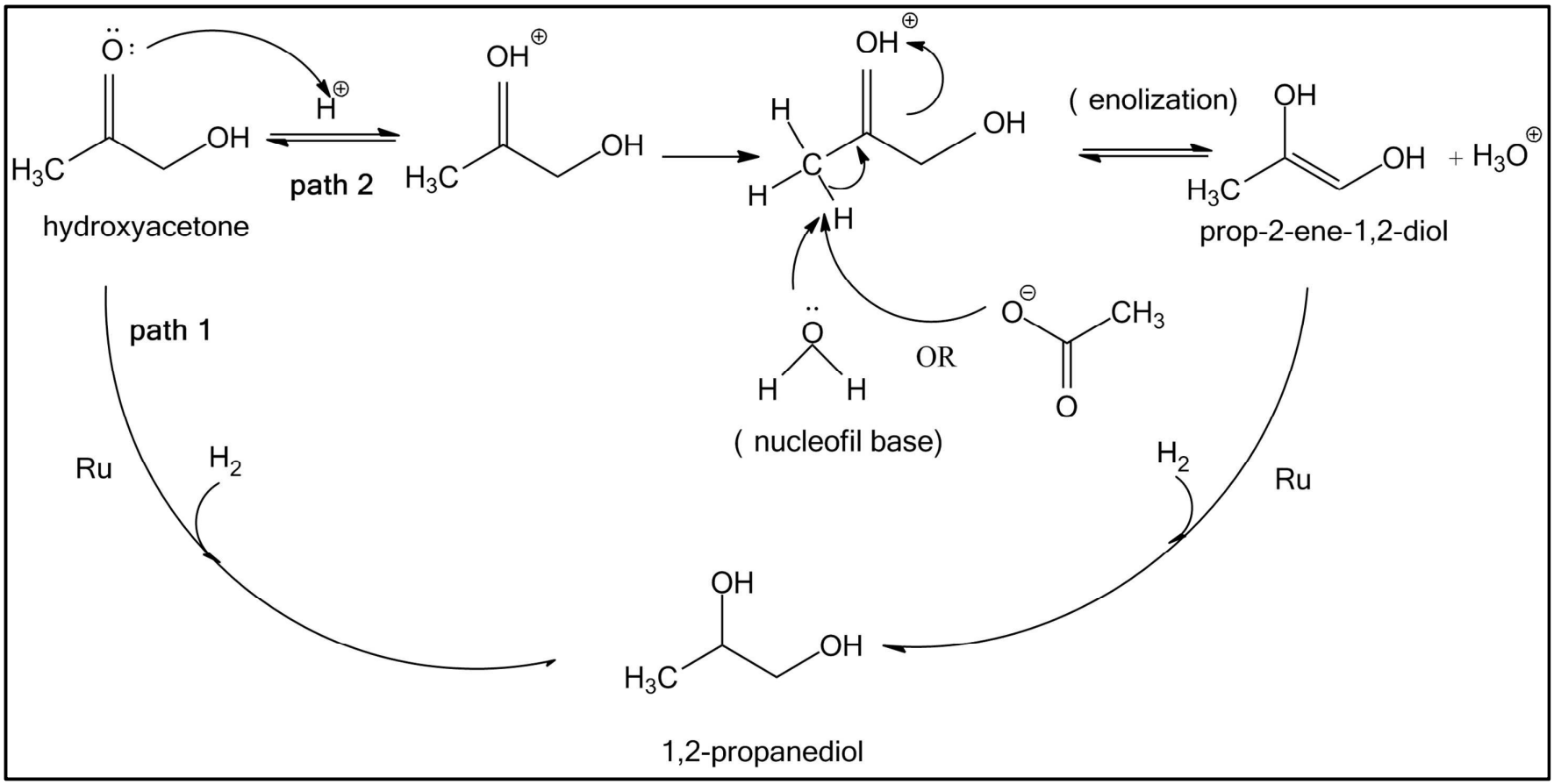

Scheme 1 Proposed reaction mechanism for the effect of acetic acid on aqueous phase hydrogenation of hydroxyacetone over 3 wt% Ru/TiO_2.

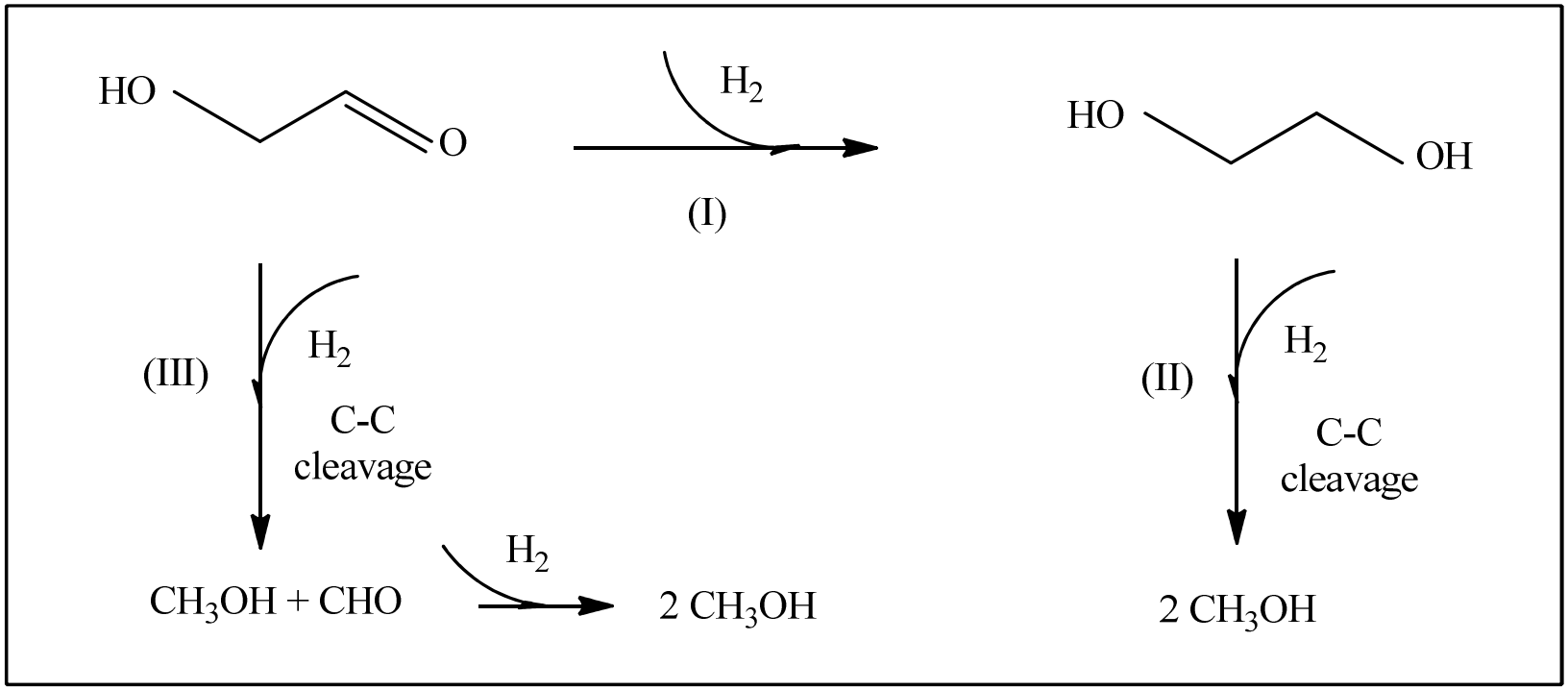

Scheme 2 Reaction pathways for formation of methanol from hydroxyacetaldehyde in hydrogenation of aqueous phase bio oil.

View Article Online
DOI: 10.1039/C7GC00367F

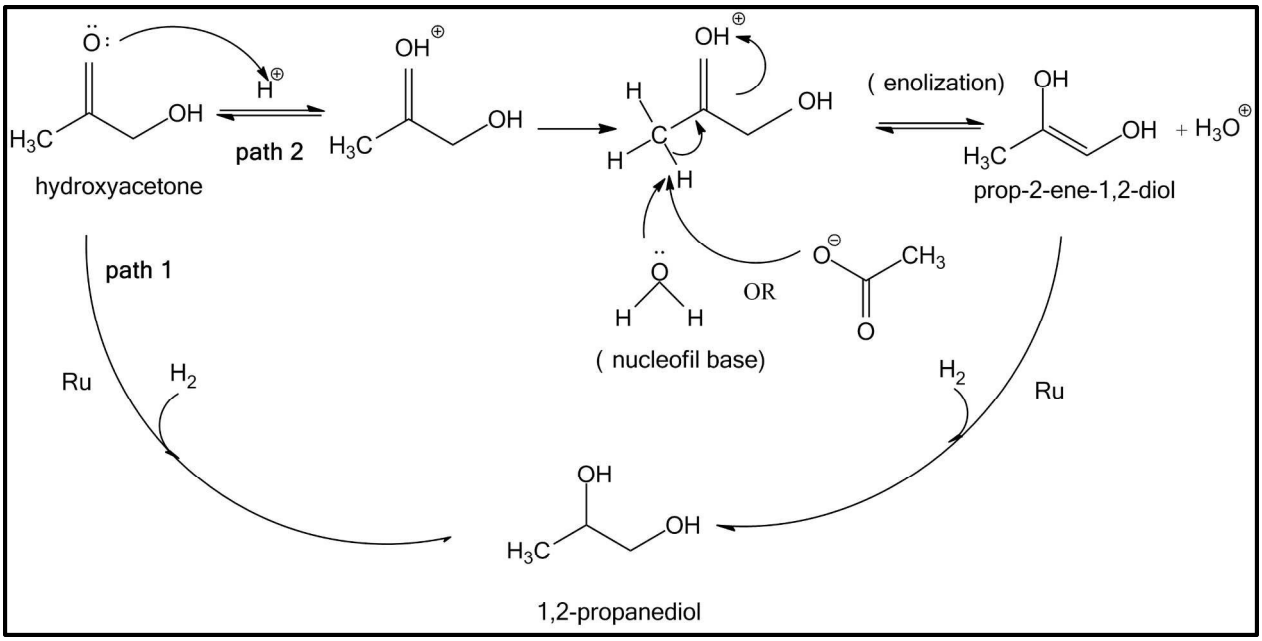

Hydroxyacetone undergoes two routes to 1,2 propanediol: 1) a direct hydrogenation route and 2) an acid catalyzed enolization route